[CANCER RESEARCH 60, 2497–2503, May 1, 2000]

Role of Extracellular Matrix Assembly in Interstitial Transport in Solid Tumors[1]

Paolo A. Netti,[2] David A. Berk,[3] Melody A. Swartz,[4] Alan J. Grodzinsky, and Rakesh K. Jain[5]

Steele Laboratory for Tumor Biology, Department of Radiation Oncology, Massachusetts General Hospital and Harvard Medical School, Boston, Massachusetts 02114 [P. A. N., D. A. B., M. A. S., R. K. J.], and Department of Electrical Engineering, Massachusetts Institute of Technology, Cambridge, Massachusetts 02139 [A. J. G.]

ABSTRACT

The extracellular matrix (ECM) may contribute to the drug resistance of a solid tumor by preventing the penetration of therapeutic agents. We measured differences in interstitial resistance to macromolecule (IgG) motion in four tumor types and found an unexpected correspondence between transport resistance and the mechanical stiffness. The interstitial diffusion coefficient of IgG was measured *in situ* by fluorescence redistribution after photobleaching. Tissue elastic modulus and hydraulic conductivity were measured by confined compression of excised tissue. In apparent contradiction to an existing paradigm, these functional properties are correlated with total tissue content of collagen, not glycosaminoglycan. An extended collagen network was observed in the more penetration-resistant tumors. Collagenase treatment of the more penetration-resistant tumors significantly increased the IgG interstitial diffusion rate. We conclude that collagen influences the tissue resistance to macromolecule transport, possibly by binding and stabilizing the glycosaminoglycan component of the ECM. These findings suggest a new method to screen tumors for potential resistance to macromolecule-based therapy. Moreover, collagen and collagen-proteoglycan bonds are identified as potential targets of treatment to improve macromolecule delivery.

INTRODUCTION

Solid tumors may evince "physiological resistance" to treatment, partly by preventing the delivery of blood-borne drugs to cancer cells (1–3). The tumor ECM[6] is one source of such resistance; tumor and stromal cells produce and assemble a matrix of collagens, proteoglycans, and other molecules that hinder the transport of macromolecules. A potentially serious flaw of novel anticancer strategies such as gene and immune therapies is their reliance on high molecular weight agents that could fail to penetrate the tumor interstitium. Although the importance of this type of physiological resistance is recognized (4, 5), no method has yet been devised to identify penetration-resistant tumors or to modify the permeability of the tumor ECM.

In mature tissues, resistance to water and solute transport is generally attributed to the amount of so-called hydrophilic ground substance, predominately GAG (6–9). However, it is now appreciated that GAG content alone does not fully account for the high transport resistance presented by many soft tissues (10–12). Tumor tissue may possess unique characteristics, attributable in part to an embryonic-like stage of development with extensive synthesis of ECM (13–15), which leads to substantial differences in composition and assembly compared with the host tissue (16–19). These differences may have important functional consequences. This study explored whether resistance to macromolecule transport in a range of tumors is related to gross differences in tumor ECM composition.

We postulated that anomalous assembly of the collagen network component and its interaction with the proteoglycan component of the tumor ECM could greatly influence the physiological barrier to macromolecule motion posed by healthy tissue ECM. To test this hypothesis, we evaluated the interstitial transport of the proteins IgG and BSA in four different tumor lines and correlated the resistance with ECM structure and composition. As a corollary to this hypothesis, we also tested whether resistance to macromolecule penetration is correlated with the mechanical stiffness of tissue, a property that is also dependent on the fibrillar collagen network and its interaction with the proteoglycans.

Materials and Methods

Tumor Preparation

Four different tumor lines were used in this study: human colon adenocarcinoma (LS174T); human glioblastoma (U87); human soft tissue sarcoma (HSTS 26T), all of which were xenografted in athymic NCr/Sed-*nu/nu* mice; and murine mammary carcinoma (MCaIV) grown in C3H mice. Tumors used for determination of mechanical and fluid transport properties, biochemical assays, and histological staining were grown s.c. in the leg. The tumors used for interstitial diffusion measurements were implanted in the s.c. region of the dorsal skin within a window chamber preparation described previously (20). All procedures were performed in accordance with the animal care guidelines of the Massachusetts General Hospital.

Mechanical and Fluid Transport Properties

The mechanical and fluid transport parameters of tumor interstitium were determined by confined compression tests following the same procedures adopted previously for cartilage (21, 22). The diameter of s.c. tumors used for these measurements ranged from 7 to 10 mm (15–20 days postimplantation). Slices of freshly excised tissue, 6 mm in diameter and 0.8–1.6-mm thick, were placed in a poly(methyl methacrylate) cylindrical confining chamber. A fitted porous polyethylene platen was placed above to maintain chemical equilibrium with the physiological saline and to allow interstitial fluid to flow freely between the tissue and the saline reservoir during the experiment. The chamber was mounted in an ultrasensitive servo-controlled materials tester (Dynastat Mechanical Spectrometer; IMASS, Hingham, MA) as described by Frank and Grodzinsky (22). Each specimen was compressed 25 μm in ramps of 15 s and allowed to relax for 20 min. Ten successive measurements were performed on each tissue slice. At each step of tissue compression, the hydraulic conductivity K was estimated from the transient stress relaxation rate by using a poroviscoelastic model (see Appendix I). Fig. 1 shows typical stress relaxation curves obtained for the four different tumors analyzed. The solid lines are the data fitting obtained with the model.

Diffusion Coefficient Measurements. The interstitial diffusion rate of tracer macromolecules was determined by FRAP with spatial Fourier analysis as described previously (23). This implementation of the FRAP method measures the mobility of fluorescently labeled molecules over a length scale of 10–100 μm. Fluorescent molecules are introduced into the interstitial space of tissue and allowed to reach a quasi-steady-state distribution (no measurable change in local concentration over a time scale of minutes). The tissue is irradiated for a duration of 50–100 ms with blue light (wavelength, 488 nm) from an argon ion laser (model 2020; Spectra-Physics, Mountain View, CA) focused to a spot size of ~40 μm diameter with an incident power of

Received 8/26/99; accepted 3/1/00.

The costs of publication of this article were defrayed in part by the payment of page charges. This article must therefore be hereby marked *advertisement* in accordance with 18 U.S.C. Section 1734 solely to indicate this fact.

[1] Supported by Outstanding Investigator Grant R35-CA56591 from the National Cancer Institute (to R. K. J.).

[2] Present address: Department of Material and Production Engineering, University of Naples 'Federico II,' Piazzale Tecchio, 80, 80125 Napoli, Italy.

[3] Present address: School of Pharmacy and Pharmaceutical Sciences, University of Manchester, Oxford Road, Manchester M13 9PL, United Kingdom.

[4] Present address: Department of Chemical Engineering, Northwestern University, Evanston, IL 60208.

[5] To whom requests for reprints should be addressed. Phone: (617) 726-4083; Fax: (617) 726-4172; E-mail: jain@steele.mgh.harvard.edu.

[6] The abbreviations used are: ECM, extracellular matrix; GAG, glycosamingoglycan; FRAP, fluorescence recovery after photobleaching; HA, hyaluronan; PAS, periodic acid Schiff.

Downloaded from http://aacrjournals.org/cancerres/article-pdf/60/9/2497/3240622/ch0900002497p.pdf by guest on 17 June 2024

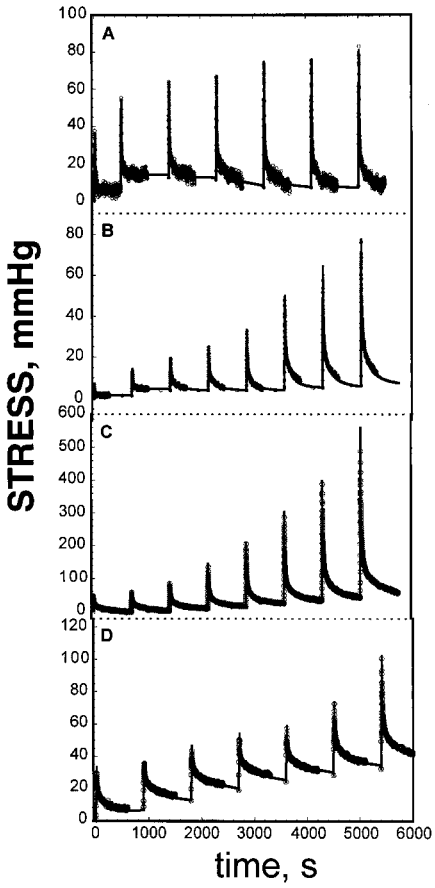

Fig. 1. Stress relaxation in confined compression for four tumor types. Typical stress relaxation curves obtained by compressing tumor tissue in a confined chamber. The HSTS 26T sarcoma (*D*) and U87 glioblastoma (*C*) tissues present a sequential increase of stress with strain, whereas for the LS174T (*A*) and MCaIV (*B*) carcinomas, the stress relaxes almost to the initial value.

~30 mW. This pulse of light creates a darkened photobleached region that subsequently dissipates as nonfluorescent and fluorescent tracer molecules mix because of diffusion. The rate of spot dissipation is quantified by image analysis, and as described previously (23), is fit to a two-component model that assumes a freely diffusing fraction of fluorescent molecules and an immobile nonspecifically bound fraction.

The diffusion coefficients were measured in tumors implanted in dorsal skinfold chambers, 15–17 days postimplantation, when each tumor had reached approximately 3–4 mm in diameter. The probe molecules (500 μg of BSA or 300 μg of IgG in 0.15 ml of sterile PBS) were administered systemically via tail vein. The IgG was a nonbinding monoclonal antibody, S1, of type IgG subclass 1. It was supplied as a gift from Hybritech (San Diego, CA) and prepared by filtration in a size exclusion chromatography column, eluted with isotonic PBS and filter-sterilized. The FRAP measurements for BSA and IgG were performed at 8 and 24 h after injection, respectively. In a different group of HSTS 26T and U87 tumors, diffusion coefficients were determined before and after collagenase treatment. Tumors were treated immediately after the initial determination of IgG mobility. Treatment consisted of a local injection of 0.3 ml of 10% collagenase (from *Clostridium*, obtained from United States Biochemical Corp., Cleveland, OH) in PBS or, for the control groups, 0.3 ml of saline alone. The diffusion coefficient was measured again 24 h after treatment, and statistical significance of the change was assessed by a two-tailed paired *t* test.

Determination of the Composition and Structure of Tumor Interstitial Matrix. The biochemical analysis for GAG, HA, and collagen content was performed on s.c. tumors of 7–8 mm diameter. Tumor tissues were surgically excised from the s.c. tissue of the hind limb, cut in three pieces, rapidly frozen in liquid nitrogen, and stored at −70°C. Each piece (40–50 mg) was then used for one of the three analyses. GAG content was determined by the method described previously (24). Tissues were finely dispersed with a homogenizer (Polytron; Brinkmann Instrument, Westbury, NY), solubilized in 1 ml of digest buffer (125 μg/ml papain in 0.1 M sodium phosphate, 5 mM Na_2 EDTA, and 5 mM cysteine-HCl, pH 6.0), and incubated for 18 h at 60°C. Sulfated GAG content was determined with the Blyscan Proteoglycan and Glycosaminoglycan assay (Biocolor Ltd., Belfast, Ireland). The total amount of GAG was determined by acids-carbazole reaction (25). The results of both measurements were expressed as equivalent mass of hexuronic acid. The amount of HA was estimated as the difference between the total and sulfated GAG measurements.

To measure total collagen content, 100 ml of papain digest were hydrolyzed in 6 N HCl at 110°C for 18 h. The hydroxyproline content of the hydrolysate was then assessed by colorimetry (26). Results are expressed as mg of collagen by reference to a standard solution of purified collagen type I (Vitrogen 100; Collagen Corp., Palo Alto, CA) in which a hydroxyproline:collagen ratio of 6.8 was measured.

Three tumors of each group were processed for histological staining. The tissue was embedded in paraffin, and 5-μm sections were cut from the fixed tissue and stained with Masson's trichrome for collagen or PAS for proteoglycans. The stained sections were observed by transmitted light microscopy with a ×40 objective, and images were recorded on color photographic film and subsequently digitized on a flatbed color scanner. The collagen stain images shown here were produced by subtracting the red from the blue channel of the digitized image (Adobe Photoshop software) so that the regions of greatest collagen staining (red absorbance) appear blue.

RESULTS

Penetrability of tumors to macromolecules correlates with tissue elasticity and hydraulic conductivity. The tumors can be classified, according to their mechanical behavior in confined compression, into "rigid" and "soft" groups. Fig. 2 shows composite equilibrium stress-strain curves for the four different tumor lines. The elastic moduli shown in Table 1 are calculated from the stress-strain curve at strains <10% (*inset* of Fig. 2). The sarcoma (HSTS 26T) and glioblastoma (U87) display sequential increases of stress with strain, as is typical of normal soft tissues (21, 22). The two carcinomas, in contrast, exhibit viscous behavior typical of a macromolecular solution rather than a well-structured solid matrix. This is also evident by the data of Fig. 1. After each successive compression, the stress measured in the two carcinomas relaxed down to the initial value, whereas for the sarcoma and glioblastoma, the stress decayed to a plateau value higher than the initial value. Fig. 2 indicates that at strains <5%, the two carcinomas show a virtually infinite compliance

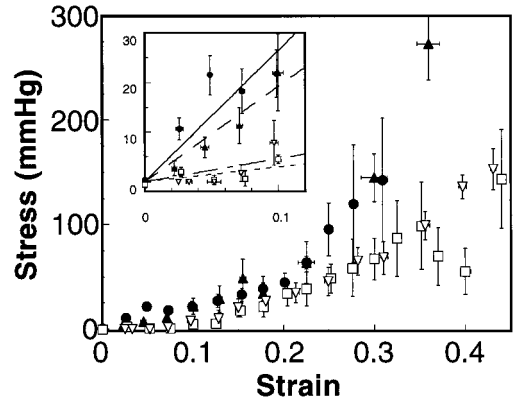

Fig. 2. Equilibrium stress-strain curve for four tumor types. The data, which are the averages of at least four tumors, are obtained by measuring the equilibrium stress generated in a confined tissue by successive compressions. The HSTS 26T sarcoma (●) and U87 glioblastoma (▲) tissues are stiffer than the LS174T (□) and MCaIV (▽) carcinomas. At low strain, the two carcinoma tissues showed virtually no increase of stress between two successive compressions (*inset*), behaving as a macromolecular solution rather that a mature well-assembled soft tissue. *Bars*, SE of all measurements at each compression step.

Downloaded from http://aacrjournals.org/cancerres/article-pdf/60/9/2497/3240622/ch0900002497p.pdf by guest on 17 June 2024

Table 1 *Mechanical and transport properties of four tumor types*

Elasticity and water flow are assessed by confined compression. Elastic moduli are obtained by a linear least-squares fit of the equilibrium stress-strain data for strains <0.1. The hydraulic conductivity K_0 of the unstressed tissue is estimated from the transient stress relaxation at each compression step. K_0 is significantly higher in HSTS 26T ($P < 0.05$; ANOVA), whereas the variation in K_0 among the other three tumor lines is not statistically significant. Data are the mean and SE of at least five tumor samples. The diffusion coefficient of IgG is measured by FRAP. Values in parentheses indicate the range of ±1 SD about the mean of at least five tumors, based on a log-normal distribution. A statistically significant dependence on tumor type is found for IgG mobility; IgG diffusivity is >2-fold higher in the two carcinomas (MCaIV and LS174T) compared with the glioblastoma (U87) and sarcoma (HSTS 26T).

Tumor	Elastic modulus mm Hg	Hydraulic conductivity (K_0) 10^{-6} cm^{-2} mm Hg^{-1} s^{-1}	Diffusion coefficient of IgG 10^{-7} cm^2 s^{-1}
MCaIV	50 ± 20	2.480 ± 1.016	1.97 (1.24–3.12)
LS174T	30 ± 10	0.450 ± 0.275	1.89 (1.29–2.77)
U87	200 ± 20	0.650 ± 0.300	0.87 (0.73–1.03)
HSTS 26T	300 ± 40	0.092 ± 0.071	0.96 (0.54–1.71)

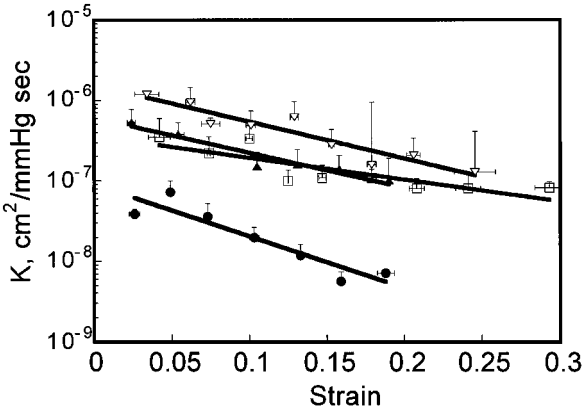

Fig. 3. Hydraulic conductivity as function of tissue deformation. The data, which are the averages of at least four different tumor tissues, are obtained by fitting the stress relaxation curves of the confined compression experiments. For all of the tissues tested, the hydraulic conductivity decreased exponentially with tissue deformation (*i.e.,* hydration). The HSTS 26T sarcoma (●) showed the highest resistance to fluid flow compared with U87 glioblastoma (▲), LS174T (□), and MCaIV (▽) carcinomas. *Bars,* SE of the *K* estimation at each compression step.

(zero slope of the stress-strain curve), indicating an absence of structural integrity (Fig. 1, *inset*). The hydraulic conductivity of the tumor tissues was evaluated by fitting the data for stress relaxation after confined compression (Fig. 1). Fig. 3 shows the tissue hydraulic conductivity for the four tumors as a function of tissue deformation (*i.e.,* hydration). As expected, the hydraulic conductivity is a strong function of tissue hydration, according to data reported for other soft tissues (27). The dependence of *K* on tissue hydration is well described by an exponential law, in agreement to that suggested in the literature for soft tissues (28) and hydrogels (29). To compare our results with those published for normal tissues, we obtained the hydraulic conductivity of tumor tissues by extrapolating the data of Fig. 3 to zero deformation. This value represents the hydraulic conductivity of unstrained tissue. By comparing our values with a compilation of published values for normal tissue (27), we found that the resistance to water flow in all but one of the tumors was lower than that of normal tissues of comparable GAG content.

We used the FRAP technique to measure the interstitial mobility of tracer proteins *in vivo* (30, 31). This technique measures protein mobility at the microscopic level so that transport in the bulk interstitial matrix is assessed separately from transvascular transport (extravasation across endothelial cells and associated perivascular matrix). In all tumors, a significant fraction (20–40%) of the macromolecules was immobile over the time-scale of ~100 s; this fraction was attributed to nonspecific binding. Comparison among the tumor groups revealed no significant difference in the nonspecific binding. The diffusion rate of the remaining unbound fraction was observed to depend on the molecule and tumor type. Fig. 4 shows the mean diffusivity of macromolecules in the four different tumor tissues. The diffusion coefficients in buffered saline solution alone (+) were also determined. The lines shown in the plot indicate the power law dependence of diffusion coefficient on macromolecule radius ($D \sim R^{-n}$) over a limited range: the free-solution data fit the Stokes-Einstein hydrodynamic model of mobility ($n = 1$); the glioblastoma/sarcoma group exhibits a much stronger dependence ($n = 3$) than the carcinoma group ($n = 1.5$). Consistent with previous studies, BSA diffused at a modestly hindered rate that did not differ significantly among tumor types. Although the mean BSA mobility in the MCaIV and LS174T groups are ~10% greater than in the U87 and HSTS 26T groups, the difference is not significant given the variance in the data (ANOVA test). However, as indicated in Table 1, the diffusion coefficient of the larger IgG molecule is significantly greater in the two carcinomas (MCaIV and LS174T) compared with the glioblastoma (U87) and sarcoma (HSTS 26T). The statistical comparison between tumor types (two-tailed unpaired *t* test) is as follows: no significant difference between LS174T *versus* MCaIV ($P = 0.88$) or between HSTS 26T *versus* U87 ($P = 0.76$); significant differences between LS174T *versus* HSTS 26T ($P = 0.0027$), MCaIV *versus* HSTS 26T ($P = 0.0023$), LS174T *versus* U87 ($P = 0.00044$), and MCaIV *versus* U87 ($P = 0.0002$). These results indicate a correlation between mechanical stiffness and resistance to movement of macromolecules of tumor tissues.

Interstitial movement of macromolecules does not correlate with GAG content. Having observed a link between tissue mechanical rigidity and resistance to the transport of the macromolecule IgG, we sought to identify a corresponding link to ECM composition. Fig. 5*A* shows the total GAG, sulfated GAG, and HA contents of each tumor. We detected no significant differences in sulfated GAG content among the tumors. However, HSTS 26T and MCaIV had a higher content of total GAG and, by inference, HA compared with both U87 and LS174T. When HA content is calculated as the difference between total and sulfated GAG, the ~2-fold greater value measured for MCaIV and HSTS 26T compared with LS174T and U87 is statistically significant ($P < 0.05$). The significant differences in HA con-

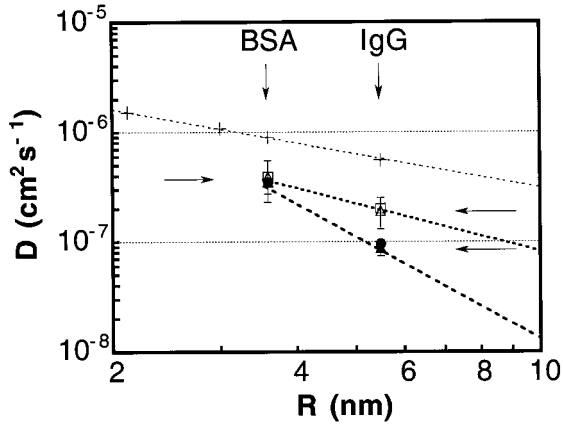

Fig. 4. Interstitial mobility of BSA (M_r 68,000) and IgG (M_r 150,000) in four tumor types and in solution. The diffusion coefficient measured by FRAP is shown on a logarithmic scale as a function of the hydrodynamic radius of the molecule. Data are the averages of at least five tumors with at least 10 evaluations performed on each tumor; *bars,* SD. The diffusion coefficients in buffered saline solution alone (+) are shown here scaled from room temperature to 34°C (by the Stokes-Einstein equation); values for lactalbumin (M_r 14,000) and ovalbumin (M_r 45,000) are also shown. ▽, MCaIV; □, LS174T; ▲, U87; ●, HSTS 26T. The *lines* shown in the plot indicate the power law dependence of diffusion coefficient on the radius of the macromolecule ($D \sim R^{-n}$).

Downloaded from http://aacrjournals.org/cancerres/article-pdf/60/9/2497/3240622/ch0900002497p.pdf by guest on 17 June 2024

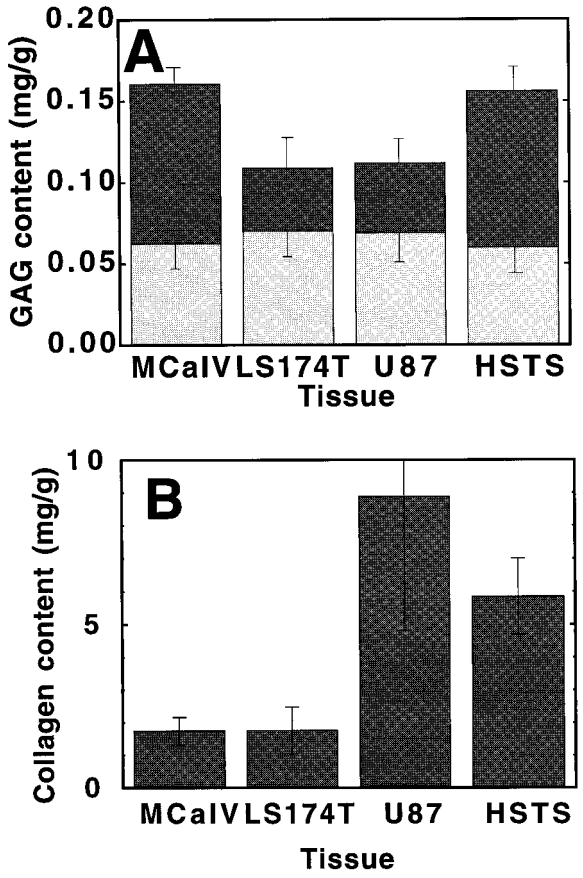

Fig. 5. Biochemical analysis of four tumor types. *A.* The tissue contents of proteoglycan (*light shading*) and HA (*dark shading*) are estimated from measurements of total and sulfated GAG, expressed in terms of equivalent mass of hexuronic acid/g wet tissue. There was no statistical difference in sulfated GAG amount among the four tumor types (ANOVA). There is ~2-fold greater value of HA measured for MCaIV and HSTS 26T compared with LS174T and U87 ($P < 0.05$). *Bars*, SE. *B*, total collagen content (hydroxyproline) in the four different tumor types. No significant differences were found between the two carcinomas (MCaIV and LS174T) or between U87 and HSTS 26T. The collagen content of U87 and HSTS 26T is significantly higher than in the two carcinomas ($P < 0.007$; ANOVA). Note that a correlation exists between the collagen content and the interstitial resistance to macromolecule transport and to compression (Table 1). *Bars*, SE.

tent, however, are not consistent with the differences seen in the functional parameters. Altogether, there is poor correlation between functional properties (resistance to transport or compression; Table 1) and GAG or HA content. On the other hand, the total collagen content of each tissue (Fig. 5*B*) does appear to mirror the measurements of elasticity and IgG mobility. The "rigid" U87 and HSTS tumors have significantly higher collagen levels compared with the "soft" carcinoma group.

Role of collagen organization on interstitial transport of macromolecules. To better understand the role of collagen on the transport resistance, we also sought to identify differences in collagen distribution among the different tumor tissues. Fig. 6 shows typical cross-sections of each tumor type stained for collagen. The U87 and HSTS 26T tumors show more intense staining for collagen compared with the two carcinomas, consistent with the biochemical data from Fig. 5. In addition, it is remarkable to note the apparent absence of any collagen organization in the two carcinomas, whereas the sarcoma and glioblastoma instead show apparently well-organized collagen lattices. A relatively collagen-rich area was evident at the border between the carcinomas and the host tissue; this "capsule" probably constitutes the major portion of collagen detected by chemical assay (Fig. 5*B*) in the carcinomas.

The histological data suggest that the organization of collagen, in addition to the absolute concentration, may be important in controlling transport. To test this hypothesis, we treated tumors of the "rigid" type with collagenase to enzymatically degrade collagen network. After collagenase treatment, the diffusivity of IgG in these low-mobility groups increased by ~2-fold (Fig. 7) to the same level observed in the two (untreated) carcinomas (values shown in Table 1). Collagenase treatment induced increases in the IgG interstitial diffusion coefficient by 100% in HSTS 26T ($P < 0.0001$) and 80% in U87 ($P < 0.05$), whereas the control saline treatment had no significant effect. This observation supports the hypothesis that an intact collagen network is required for tissue to effectively resist penetration by macromolecules.

DISCUSSION

The ECM acts as a dispersive filter, controlling the composition of extracellular fluid and the rate of molecular trafficking. This control is mediated by a synergistic interaction among ECM constituents. Although proteoglycans are essential to the physiological functions of the ECM, our data support the view that proteoglycans require a stabilizing solid matrix to exert their full transport-limiting effect. It is widely accepted that in mature normal tissues, the collagen network provides the structural and mechanical integrity of the ECM (12, 32), whereas proteoglycans anchored to the network regulate the movement of fluid and solute (12, 27) and provide resistance to compressive forces (12, 33). Indeed, the importance of a structural matrix is made evident by the observation that macromolecular solutions of GAG offer transport resistance orders of magnitude lower than most tissues with equal proteoglycan content (27). Interestingly, the hydraulic conductivities of LS174T and MCaIV tumors are comparable with those of GAG solution of the same concentration, whereas the hydraulic conductivity of HSTS tumor is comparable with that of soft tissue with the same GAG content (27). Hence, this suggests that tumors rich in HA are not necessarily resistant to fluid and macromolecule penetration unless the HA is stabilized by a collagen matrix.

Tissue collagen composition alone is unlikely to completely control the resistance to transport of macromolecules. It has been reported that collagen gels *in vitro* exhibit resistances to transport of fluid (34) and macromolecules (35), which are significantly less than that shown by tissues having the same collagen composition. Our results suggest that the organization of the collagen and the combination of collagen and proteoglycans contribute significantly to the interstitial transport resistance. This hypothesis is also supported by *in vitro* data showing that composite gels of collagen and hyaluronic acid have a higher resistance to macromolecular transport than gels of collagen or hyaluronic acid alone (36).

The transport barrier posed by the ECM is particularly important in tumor because it may prevent the penetration of therapeutic agents. To assess the role of ECM composition and organization on the penetration of high molecular weight therapeutic agents, we evaluated the diffusion hindrance of probe macromolecules (BSA and nonspecific IgG) within the tumor interstitium *in vivo*. The data show that resistance to IgG penetration is related to tumor rigidity and to collagen organization, as suggested by histology (Fig. 6) and tested by collagenase treatment (Fig. 7). In contrast, total tissue content of proteoglycans did not vary substantially among the four tumor types, and modest differences in HA and total GAG did not correspond to the observed differences in the tissue functional properties. This result is supported by published observations of direct intratumoral infusion of macromolecular solutions in the two of the same tumor types used for the present study. Boucher *et. al* (37) reported that when a solution of Evans-blue-stained albumin was infused into the center of LS174T tumors at flow rates of 0.1 μl/min for 90 min, the dye flowed radially

Downloaded from http://aacrjournals.org/cancerres/article-pdf/60/9/2497/3240622/ch0900002497p.pdf by guest on 17 June 2024

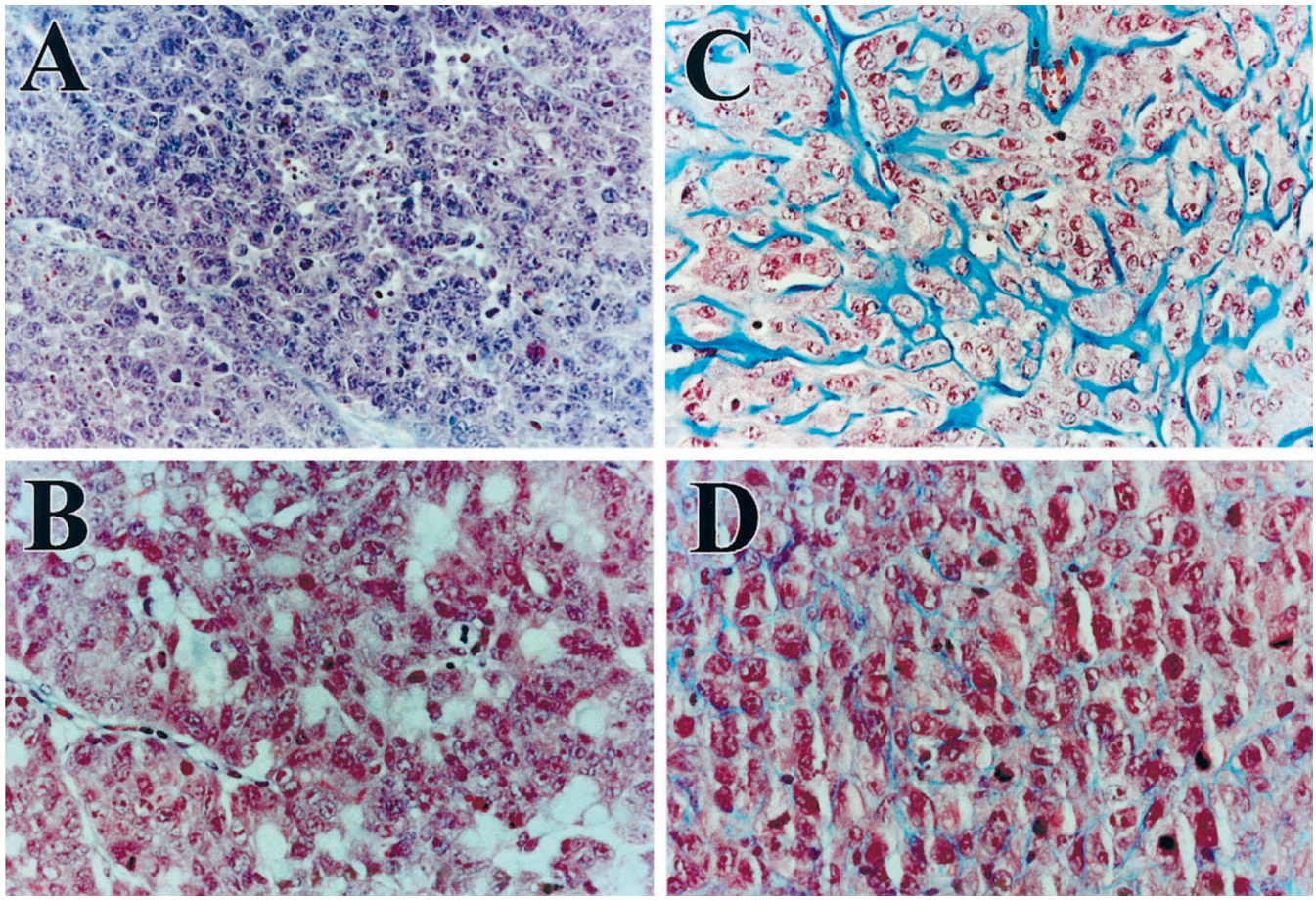

Fig. 6. Histological staining of collagen in the four different tumors. The collagen staining is weak and diffuse in the MCaIV (*A*) and LS174T (*B*) compared with U87 (*C*) and HSTS 26T (*D*). The most important feature to note is the lack of an interconnected collagen network in the two carcinomas; collagen is associated with blood vessels. Compared with the carcinoma tissues, the U87 and HSTS 26T sections show well-organized interconnected collagen lattices surrounding cell clusters. The HSTS 26T sarcoma has a finer network structure compared with the U87 tissue.

outward from the needle tip into a spherical volume of 2.5–4.0 mm diameter. In contrast, using the same infusion protocol in HSTS 26T tumors, they observed a greater resistance to flow, indicated by a nonuniform distribution of the dye and significant accumulation in a narrow region around the infusion needle. These data show that tumors with a well-defined collagen network are more resistant to penetration by macromolecular drugs compared with tumors that exhibit a loose collagen network. We propose that macromolecule access to tumor tissue is dominated by deficiencies in collagen assembly and relatively insensitive to variations in GAG content.

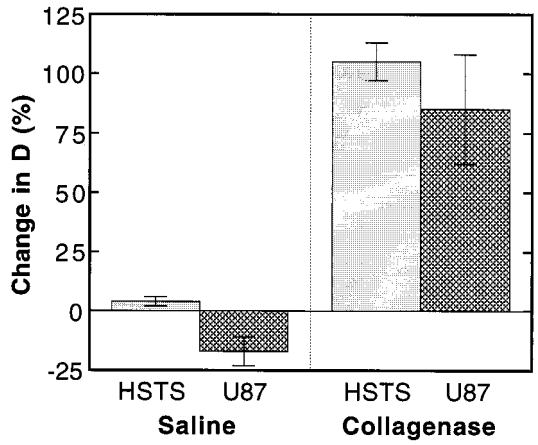

Fig. 7. Effect of collagenase treatment on IgG mobility in U87 and HSTS 26T. Measurements were performed 24 h (pretreatment diffusion coefficient) and 48 h (24 h after treatment) after i.v. administration of fluorescein-labeled IgG. There were four tumors in each collagenase-treated group and three tumors in each saline-treated control group. At least 10 FRAP measurements were performed in each tumor. *Bars*, SD.

Degeneration of the collagen network and a resulting compromised physiological function may be general features of tumors. Proteolytic remodeling of the ECM may be a requirement for tumor angiogenesis, growth, invasion, and metastasis (38). Moreover, molecular defects in the assembly process may be associated with the loss of normal cellular growth regulation mechanisms. For example, β_1 integrin fibronectin receptor expression such as $\alpha_5\beta_1$ affects ECM organization and is altered in neoplastic cells (39–42). Regardless of the reason, ECM organization is often abnormal in tumors (16, 17, 19).

The results identify measurable tumor characteristics that could be useful in predicting penetration by therapeutic macromolecules. We suggest that simple histological staining of tumor tissue biopsies can be used to assess the feasibility of therapeutic approaches requiring macromolecule penetration. Delivery of high molecular weight agents should be facilitated in tumors with poorly organized and loosely interconnected collagen networks. In this study, both types of carcinoma exhibit deficient collagen assembly, but in general this trait is probably determined by the interaction of both neoplastic and host cells. Particularly in tumors of epithelial origin, host stromal cells are involved in the production and organization of matrix molecules (43). Hence, the transport properties of the

Downloaded from http://aacrjournals.org/cancerres/article-pdf/60/9/2497/3240622/ch0900002497p.pdf by guest on 17 June 2024

tumor interstitial matrix likely depend on the site of tumor growth as well as the tumor type.

If "molecular medicine" is to have an impact on cancer treatment, it will be necessary to confront and overcome the delivery problems affecting these novel agents. Modification of the tumor ECM is one strategy that could promote better delivery. Hyaluronidase treatment reportedly enhances chemotherapy of some tumors. However, this approach may not be applicable in systemic treatments, and it is possible that the chemosensitizing effect occurs by mechanisms other than enhanced permeability of the ECM (44). This study points to collagen as a likely target for modification. A tumor with a well-developed collagen network could be considered "physiologically resistant" to macromolecule-based therapies, but this resistance could be reduced by treatments that reverse or inhibit collagen production and assembly.

ACKNOWLEDGMENTS

We thank Drs. Yves Boucher, Alain Pluen, and Saroja Ramanujan for many helpful discussions.

APPENDIX I

The proviscoelastic model used to describe the fluid transport and the mechanical properties of tumor tissue is similar to that proposed by Mak (45) but with a more suitable constitutive equation. Following the approach largely used to describe the biomechanics of cartilage (22, 28), we consider the tumor tissue as a biphasic medium composed of a solid viscoelastic matrix (ECM) and a fluid phase (interstitial fluid; Refs. 46 and 47). The theory assumes that the total stress acting on the tissue is the sum of the stress acting on the solid matrix and the stress acting on the interstitial fluid:

$$\underline{\underline{\sigma}}^T = \underline{\underline{\sigma}}^s + \underline{\sigma}^f$$

The momentum balance for the tissue under the hypothesis of negligible inertial forces is:

$$\nabla \cdot \underline{\underline{\sigma}}^T = \underline{0} \tag{A1}$$

For the momentum balance of the fluid phase, it is assumed that the divergence of the fluid stress is balanced by the fractional drag force, *i.e.*:

$$\nabla \cdot \underline{\underline{\sigma}}^f = \zeta\left(\underline{v}^f - \frac{\partial \underline{u}}{\partial t}\right)$$

where ζ is the drag coefficient; $\underline{u}$ is the displacement of the solid phase; $\underline{v}^f$ and $\partial\underline{u}/\partial t$ are the local velocities of the fluid and solid phase, respectively. This equation can also be written as:

$$\phi\left(\underline{v}^f - \frac{\partial \underline{u}}{\partial t}\right) = -K\nabla p \tag{A2}$$

where ϕ is the tissue volume fraction and K ($= \phi^2/\zeta$) is the tissue hydraulic conductivity (a measure of the resistance to water flow). Eq. A2 represents a generalized Darcy's law, where the hydrostatic pressure gradient acts on the relative velocity between the solid and liquid phases, and it expresses the basic concept of the biphasic theory, *i.e.*, the coupling between stress and fluid movement. Indeed, if the divergence of the solid stress tensor ($\nabla \cdot \sigma^s$) is not zero, then a hydrostatic pressure gradient arises, leading to a relative motion between the solid and fluid phase.

The mass balance equations for the fluid and solid phase, respectively, are:

$$\frac{\partial \phi}{\partial t} + \nabla \cdot (\phi \underline{v}^f) = 0 \tag{A3}$$

and

$$-\frac{\partial \phi}{\partial t} + \nabla \cdot \left((1-\phi)\frac{\partial \underline{u}}{\partial t}\right) = 0, \tag{A4}$$

To complete the description, the constitutive equations for the fluid and solid phases are needed. Because the average fluid velocity field ($\underline{v}^f$) is irrotational (46), it can be described as a perfect fluid, *i.e.*:

$$\underline{\underline{\sigma}}^f = -\phi p \underline{\underline{I}}$$

For the solid matrix, we assume a viscoelastic behavior that, under the hypothesis of small strain, can be described in general terms as:

$$\underline{\underline{\sigma}}^s = -(1-\phi)p\underline{\underline{I}} + 2\mu\underline{\underline{\varepsilon}} + \lambda e\underline{\underline{I}} + c\int_{-\infty}^{t} m(t-\xi)\frac{\partial}{\partial \xi}(\underline{\underline{\varepsilon}} + e\underline{\underline{I}})d\xi \tag{A5}$$

where $\underline{\underline{\varepsilon}}$ is the deformation tensor, e is the dilatation of the tissue ($=|\nabla\cdot\underline{\underline{\varepsilon}}|$), μ and λ are the Lamé constant, $m(t)$ is the memory function of the material, and c is a material constant. The first term is the Laplacian multipliers to take into account the effect of hydrostatic pressure on the solid matrix; the second and third terms represent the elastic components of the mechanical response of the material; and the fourth term takes into account the effects of viscoelasticity of the matrix. The memory function can be expressed in terms of the spectrum of relaxation times of the material [H]:

$$m(t) = \int_0^\infty \frac{H(\varphi)}{\varphi} e^{-t/\varphi} d\varphi$$

We assumed the ECM to be a linear viscoelastic solid with a spectrum of relaxation times:

$$\begin{cases} H(\varphi) = \dfrac{\tau}{\delta} & \lambda \in [\tau-\delta,\ \tau+\delta] \\ H(\varphi) = 0 & \lambda \notin [\tau-\delta,\ \tau+\delta] \end{cases} \tag{A6}$$

where $\tau - \delta$ and $\tau + \delta$ are the shortest and the longest relaxation times, respectively. The parameter δ is a measure of the range of the relaxation times. Similar forms of the relaxation spectrum have been used to describe the viscoelasticity of soft tissues such as ligaments and skin (48).

Combining equations A1–A4 with the constitutive equations of the fluid and solid phases, the governing equation in the Laplace space for a uniaxial geometry results:

$$\frac{d^2\underline{u}}{dz^2} = f(s)\underline{u} \tag{A7}$$

where

$$f(s) = \frac{s}{K\left(H + 2c\ln\left(\dfrac{1+s(\tau+\varepsilon)}{1+s(\tau-\varepsilon)}\right)\right)} \tag{A8}$$

The boundary equations are:

$$\begin{cases} \underline{u}(t,\ 0) = \Delta\dfrac{t}{t_o} & \text{for } 0 \le t \le t_o \\ \underline{u}(t,\ 0) = \Delta & \text{for } t \ge t_o \\ \underline{u}(t,\ h) = 0 & \forall\, t \end{cases} \tag{A9}$$

where Δ is compression displacement at each step ($\sim$25 μm), t_0 is the time required for the compression step (15 s), and h is the thickness of the specimen.

Eq. A8 with the boundary conditions (A9) is integrated in the Laplace space and then numerically converted in the time domain to fit the experimental data and estimate the parameters K, H, c, and δ.

Downloaded from http://aacrjournals.org/cancerres/article-pdf/60/9/2497/3240622/ch0900002497p.pdf by guest on 17 June 2024

APPENDIX II

c	viscoelastic material parameter	(mm Hg)
D	interstitial diffusion coefficient	(cm^2/s)
Do	diffusion coefficient in solution	(cm^2/s)
δ	range of relaxation times of the solid matrix	(s)
Δ	compression displacement	(μm)
$\underline{\underline{\varepsilon}}$	matrix deformation tensor	
e	solid matrix dilatation	
$H(\varphi)$	spectrum of relaxation time of the solid matrix	
Hm	elastic consolidation modulus	(mm Hg)
$\underline{\underline{I}}$	unity tensor	
K	interstitial hydraulic permeability	(cm^2/mm Hg-s)
μ, λ	Lamé constants for solid matrix	(mm Hg)
$m(t)$	memory function of the solid matrix	
p	interstitial fluid pressure	(mm Hg)
ϕ_T	tissue fluid fraction	
$\underline{\underline{\sigma}}^s$	tissue stress tensor	(mm Hg)
$\underline{\underline{\sigma}}^s$	solid stress tensor	(mm Hg)
$\underline{\underline{\sigma}}^f$	fluid stress tensor	(mm Hg)
ζ	solid matrix-interstitial fluid drag coefficient	(mm Hg-s/cm^2)
t	time	(s)
t_o	time of the compression ramp	(s)
$\underline{u}$	solid matrix displacement	(μm)
$\underline{v}_f$	interstitial fluid velocity	(μm/s)
z	spatial coordinates	(cm)

REFERENCES

1. Jain, R. K. Delivery of molecular medicine to solid tumors. Science (Washington DC), *271:* 1079–1080, 1996.
2. Jain, R. K. The next frontier of molecular medicine: delivery of therapeutics. Nat. Med., *4:* 655–657, 1998.
3. Jain, R. K. 1995 Whitaker Lecture: Delivery of molecules, particles and cells to solid tumors. Ann. Biomed. Eng., *24:* 457–473, 1996.
4. Swabb, E. A., Wei, J., and Gullino, P. M. Diffusion and convection in normal and neoplastic tissues. Cancer Res., *34:* 2814–2822, 1974.
5. Dedrick, R. L., and Flessner, M. F. Pharmacokinetic problems in peritoneal drug administration: tissue penetration and surface exposure. J. Natl. Cancer Inst., *89:* 480–487, 1997.
6. Mow, V. C., Mak, A. F., Lai, W. M., Rosenberg, L. C., and Tang, L. H. Viscoelastic properties of proteoglycan subunits and aggregates in varying solution concentrations. J. Biomech., *17:* 325–338, 1984.
7. Ogston, A. G., and Sherman, T. F. Effect of hyaluronic acid upon diffusion of solutes and flow of solvent. J. Physiol., *156:* 67–74, 1961.
8. Auckland, K., and Nicolaysen, G. Interstitial fluid volume: local regulatory mechanisms. Physiol. Rev., *61:* 556–643, 1981.
9. Comper, W. D., and Laurent, T. C. Physiological function of connective tissue polysaccharides. Physiol. Rev., *58:* 255–315, 1978.
10. Jackson, G. W., and James, D. F. The hydrodynamic resistance of hyaluronic acid and its contribution to tissue permeability. Biorheology, *19:* 317–330, 1982.
11. Levick, J. R. Relation between hydraulic resistance and composition of the interstitium. *In:* N. C. Staub, J. C. Hogg, and A. R. Hargens (eds.), Interstitial-Lymphatic Liquid and Solute Movement, Vol. 13, pp. 124–133. Basel: Karger, 1987.
12. Winlove, C. P., and Parker, K. H. The physiological function of the extracellular matrix. *In:* R. K. Reed, G. A. Laine, J. L. Bert, C. P. Winlove, and N. McHale (eds.), Interstitium, Connective Tissue and Lymphatics, pp. 137–165. London: Portland Press, 1995.
13. Iozzo, R. V. Biology of a disease–proteoglycans: structure, function, and role in neoplasia. Lab. Investig., *53:* 373–396, 1985.
14. Sakamoto, S., and Sakamoto, M. Degradative processes of connective tissue proteins with special emphasis on collagenolysis and bone resorption. Mol. Aspects Med., *10:* 301–428, 1988.
15. Ronnov-Jessen, L., Petersen O. W., and Bissell, M. J. Cellular changes involved in conversion of normal to malignant breast: importance of the stromal reaction. Physiol. Rev., *76:* 69–125, 1996.
16. Liotta, L. A., and Rao, C. N. Role of extracellular matrix in cancer. Ann. NY Acad. Sci., *460:* 333–344, 1985.
17. Dvorak, H. F. Tumors. Wounds that do not heal. N. Engl. J. Med., *315:* 1650–1659, 1986.
18. Labat-Robert, J., and Robert, L. Interaction between structural glycoproteins and collagens. *In:* M. E. Nimmi (ed.), Collagen, Vol. 1, pp. 173–186. Boca Raton, FL: CRC Press, 1988.
19. Line, S. R., Torloni, H., and Junqueira, L. C. Diversity of collagen expression in the pleomorphic adenoma of parotid gland. Virchows Archiv. A Pathol. Anat. Histopathol., *414:* 477–483, 1989.
20. Leunig, M., Yuan, F., Menger, D. M., Boucher, Y., Goetz, A. F., Messmer, K., and Jain, R. K. Angiogenesis, microvascular architecture, microhemodynamics, and interstitial fluid pressure during early growth of human adenocarcinoma LS174T in SCID mice. Cancer Res., *52:* 6553–6560, 1992.
21. Mow, V. C., Kuei, S. C., Lai, W. M., and Armstrong, C. G. Biphasic creep and stress relaxation of articular cartilage in compression: theory and experiments. J. Biomech. Eng., *102:* 73–84, 1980.
22. Frank, E. H., and Grodzinsky, A. J. Cartilage electromechanics. I. Electrokinetic transduction and the effect of electrolyte pH and ionic strength. J. Biomech., *20:* 615–627, 1987.
23. Berk, D. A., Yuan, F., Leunig, M., and Jain, R. K. Fluorescence photobleaching with spatial Fourier analysis: measurement of diffusion in light-scattering media. Biophys. J., *65:* 2428–2436, 1993.
24. Sah, R. L., Kim, Y-J., Doong, J. H., Grodzinsky, A. J., and Plaas, A. J. Biosynthetic response of cartilage explants to dynamic compression. J. Orthop. Res., *7:* 619–636, 1989.
25. Bitter, T., and Muir, H. M. A modified uronic acid carbazole reaction. Anal. Biochem., *4:* 330–334, 1962.
26. Woessner, J. F. The determination of hydroxyproline in tissue and protein samples containing small proportions of the imino acid. Arch. Biochem. Biophys., *93:* 440–447, 1961.
27. Levick, J. R. Flow trough interstitium and other fibrous matrices. Q. J. Exp. Physiol., *72:* 409–437, 1987.
28. Mow, V. C., Holmes, M. H., and Lai, W. M. Fluid transport and mechanical properties of articular cartilage: a review. J. Biomech., *17:* 377–394, 1984.
29. Johnson, E. M., and Deen, W. M. Hydraulic permeability of agarose gels. AlChE J., *42:* 1220–1224, 1996.
30. Chary, S. R., and Jain, R. K. Direct measurement of interstitial diffusion and convection of albumin in normal and neoplastic tissues using fluorescence photobleaching. Proc. Natl. Acad. Sci. USA, *86:* 5385–5389, 1989.
31. Berk, D. A., Yuan, F., Leunig, M., and Jain, R. K. Direct *in vivo* measurement of targeted binding in a human tumor xenograft. Proc. Natl. Acad. Sci. USA, *94:* 1785–1790, 1997.
32. Barocas, V. H., and Tranquillo, R. T. An anisotropic biphasic theory of tissue-equivalent mechanics: the interplay among cell traction, fibrillar network deformation, fibril alignment, and cell contact guidance. J. Biomech. Eng., *119:* 137–145, 1997.
33. Silver, F. H. Biological Materials. Structure, Mechanical Properties, and Modelling of Soft Tissues. New York: New York University Press, 1987.
34. Jackson, R. L., Bush, S. J., and Cardin, A. D. Glycosaminoglycans: molecular properties, protein interactions, and role in neoplasia. Physiol. Rev., *71:* 481–539, 1991.
35. Saltzman, W. M., Radomsky, M. L., Whaley, K. J., and Cone, R. A. Antibody diffusion in human cervical mucus. Biophys. J., *66:* 508–515, 1994.
36. Shenoy, V., and Rosenblatt, J. Diffusion of macromolecules in collagen and hyaluronic acid. Rigid-rod-flexible polymer, composite matrices. Macromolecules, *28:* 8751–8758, 1995.
37. Boucher, Y., Brekken, C., Netti, P. A., and Jain, R. K. Intratumoral infusion of fluid: estimation of hydraulic conductivity and implication for the delivery of therapeutic agents. Br. J. Cancer, *78:* 1442–1448, 1998.
38. Coussens, L. M., and Werb, Z. Matrix metalloproteinases and the development of cancer. Chem. Biol., *3:* 895–904, 1996.
39. McDonald, J. A. Extracellular matrix assembly. Annu. Rev. Cell Biol., *4:* 183–207, 1988.
40. Plantefaber, L. C., and Hynes, R. O. Changes in integrin receptors on oncogenically transformed cells. Cell, *56:* 281–290, 1989.
41. Juliano, R. L. The role of β1 integrins in tumors. Cancer Biol., *4:* 277–283, 1993.
42. Ruoslahti, E. Fibronectin and its $\alpha 5\beta 1$ integrin receptor in malignancy. Invasion Metastasis, *14:* 87–97, 1994.
43. Knudson, W., Biswas, C., and Toole, B. P. Interactions between human tumor cells and fibroblasts stimulate hyaluronate synthesis. Proc. Natl. Acad. Sci. USA, *81:* 6767–6771, 1984.
44. Croix, B. S., Rak, J. W., Kapitain, S., Sheehan, C., Graham, C. H., and Kerbel, R. S. Reversal by hyaluronidase of adhesion-dependent multicellular drug resistance in mammary carcinoma cells. J. Natl. Cancer Inst., *88:* 1285–1296, 1996.
45. Mak, A. F. The apparent viscoelastic behavior of articular cartilage. The contributions from the intrinsic matrix viscoelasticity and interstitial flows. J. Biomech. Eng., *108:* 123–130, 1986.
46. Netti, P. A., Baxter, L. T., Boucher, Y., Skalak, R., and Jain, R. K. Macro and microscopic fluid transport in living tissues: application to solid tumors. AlChE J., *43:* 818–834, 1997.
47. Netti, P. A., Baxter, L. T., Boucher, Y., Skalak, R., and Jain, R. K. Time-dependent behavior of interstitial fluid pressure in solid tumors: implication for drug delivery. Cancer Res., *55:* 5451–5458, 1995.
48. Fung, Y. C. Biomechanics. Mechanical Properties of Living Tissues. New York: Springer-Verlag, 1993.

Downloaded from http://aacrjournals.org/cancerres/article-pdf/60/9/2497/3240622/ch0900002497p.pdf by guest on 17 June 2024